Unveiling the Impact of Distinct Melanosome Arrangements on the Attenuation of Cancer-Inducing Ultraviolet Radiation

Gladimir V. G. Baranoski[1], Senior Member, IEEE, Tenn F. Chen[2] and Spencer R. Van Leeuwen[1]

***Abstract*— The exposure of human skin to ultraviolet radiation (UVR) can trigger a wide array of biological responses, including photocarcinogenesis. Melanin, either in colloidal form or encapsulated into melanosomes, is known to be the main UVR attenuation substance acting within the cutaneous tissues. Although many studies have addressed the protective role of this pigment against the harmful effects of UVR exposure, the impact of different melanosome arrangements on the mitigation of these effects remains to be quantitatively verified. The difficulties to resolve this open question can be mainly attributed to the intrinsic practical limitations of *in vivo* and *in vitro* experiments involving skin specimens. In this paper, we describe controlled *in silico* experiments that allowed us to overcome such limitations and provide quantitative evidence for the clarification of this question. Besides contributing to a more robust understanding of the physiological parameters associated with cutaneous UVR attenuation, our findings can be incorporated into the development of more effective strategies for the evaluation of individuals' susceptibility to UVR exposure. Such strategies are essential for the prevention of UVR-induced pathologies, particularly skin cancer.**

***Index Terms*— ultraviolet radiation, melanin, melanosome, skin cancer, sieve and detour effects, predictive simulation.**

I. Introduction

The ultraviolet radiation (UVR) impinging on human skin, more specifically in the regions of the light spectrum termed UVB (280-315 nm) and UVA (315-380 nm) [1], can trigger a myriad of photobiological processes. Although some of these processes, such as vitamin D synthesis and nitrite oxide induction [2], [3], can result in benefits for human health, others, like erythema (sunburn) and photoaging [2], [3], have detrimental consequences. Moreover, overexposure to UVR can elicit photobiological processes, such as photoimmunosupression and photocarcinogenesis [2], [4], that can lead to life-threatening conditions such as melanoma skin cancer.

After UVR penetrates the cutaneous tissues, it is subjected to light attenuation (scattering and absorption) events. When it is absorbed, this may start or intensify specific photobiological processes, like those mentioned above, depending on the absorber and the wavelength of the impinging UVR. For example, DNA strongly absorbs light in the UVB spectral region [5]. This may result in DNA damage, which, in turn, can cause mutations that may give rise to tumours [4].

*This work was supported in part by the Natural Sciences and Research Council of Canada (NSERC) under Grant 238337.

[1] Gladimir V. G. Baranoski and Spencer R. Van Leeuwen are with the Natural Phenomena Simulation Group, School of Computer Science, University of Waterloo, 200 University Avenue, Waterloo, Ontario, N2L 3G1, Canada. gvgbaran@cs.uwaterloo.ca

[2] Tenn F. Chen is with Google Inc., 1600 Amphitheatre Pkwy, Mountain View, CA 94043, USA.

Fig. 1. Sketches illustrating distinct melanosome arrangements. Left: large, individually dispersed melanosomes. Center: small melanosomes aggregated into melanosome complexes. Right: smaller melanosomes aggregated into less compact complexes.

Although the peak of UV-induced DNA damage has been shown to lie within the UVB region [4], the contribution of UVA to indirect DNA damage should be noted as well [6]. Upon UVA exposure, melanin, the strongest UV-absorbing pigment found in human skin [7], can generate reactive oxygen species that, in high levels, may induce single strand DNA breaks [3], [6]. It is worth noting that UVA-rich lamps are often used in the indoor tanning industry. This may explain the relatively high incidence of all types of skin cancer in individuals who are frequent users of tanning beds [3], [8].

Despite the deleterious effects that can result from melanin overexposure to UVR, epidemiological data strongly supports its more prominent photoprotective role [6], [9], [10]. Light attenuation by melanin, either through absorption or scattering mechanisms, depends not only on the amount of this pigment present in the cutaneous tissues, but also on its distribution pattern [11], [12], [13]. Melanin is synthesized by melanocyte cells in the stratum basale (the innermost epidermal layer) where it is preferentially concentrated [11]. As the epidermal cells move upward, it is distributed throughout the full thickness of the upper epidermal layers [14].

The two forms of melanin found in human skin, the dominant brown-black eumelanin and the yellow-red pheomelanin, may be present in colloidal form or clustered within organelles called melanosomes [9]. It has been observed [14], [15], [16], [17] that the presence of melanosomes within the cutaneous tissues can be characterized by distinct arrangements. More specifically, they can occur in large sizes and individually dispersed, or in small sizes forming groups surrounded by a transparent membrane (Fig. 1). These groups, called melanosome complexes, are approximately spherical in shape and their size is inversely proportional to the size of the encapsulated melanosomes [15], [16], [17].

It has been suggested that large and individually dispersed melanosomes can provide a superior mechanism of protection by attenuating the impinging UVR more efficiently [10], [15], [16], [18], [19], [20]. To the best of our knowledge, however, such a speculation has been mostly based on

978-1-5386-3646-6/18/$31.00 ©2018 IEEE

circumstantial evidence. For example, it was observed [15], [21] that Australian Aborigines, whose melanosomes are individually dispersed [21], are subject to lower incidence of skin cancer caused by UVR exposure than their fellow Australians of European origin, whose melasomes are aggregated into melanosome complexes [15].

The lack of quantitative evidence to explain this protective mechanism can be mainly attributed to the fact that *in vivo* experiments involving direct exposure to UVR may pose risks to the subjects' health. Although one could resort to *in vitro* experiments, the procedures employed to collect and prepare skin samples would change their optical properties. Moreover, the execution of controlled *in vivo* or *in vitro* experiments involving the modification of melanosome arrangements *in situ*, without altering the other biophysical characteristics of the specimen at hand, is unfeasible using the currently available technology.

In this work, we performed the first systematic investigation of the impact of distinct melanosome arrangements on UVR attenuation. To overcome the *in vivo* and *in vitro* experimental limitations outlined above, we performed controlled *in silico* experiments. These experiments were carried out using biophysical data provided in the literature and a first-principles light transport model for human skin, known as HyLIoS (*H*yperspectral *L*ight *I*mpingement on *S*kin), whose fidelity has been extensively evaluated through comparisons of its predictions against measurements obtained from real skin specimens [22]. Our experimental results, which were obtained considering a broad range of pigmentation variations, quantitatively demonstrate the different levels of UVA and UVB absorption efficiency provided by distinct melanosome arrangements.

II. Investigation Framework

The HyLIoS model [22] employs a stochastic formulation that incorporates all main light absorbers (keratin, DNA, uranic acid, melanins, functional and disfunctional hemoglobins, beta-carotene, bilirubin, lipids and water) and scatterers (cells, fibers, fibrils, melanosomes and melanosome complexes) acting within the cutaneous tissues. Moreover, HyLIoS explicitly accounts for the melanosomes' particle nature and their different arrangements within the epidermal layers. Hence, it enables the computation of light absorptance within each of these layers considering the occurrence of melanin in colloidal and aggregated forms.

In order to compare the impact of distinct melanosome arrangements on UVR attenuation, we have considered the melanosomes located in the stratum basale (SB). This choice was motivated by two aspects. First, in normal skin, the majority of the encapsulated melanin is located within this layer [6], [11]. Second, it is considered a critical area for photocarcinogenesis since its cells can persist and pass on their UV-induced mutations to daughter cells [8].

The data used to represent the three melanosome arrangements (A, B and C) examined in this investigation are provided in Table I. Within HyLIoS' formulation, melanosomes are modeled as prolate spheroids employing dimensions

TABLE I

Data employed in the characterization of the three melanosome arrangements considered in this investigation.

Arrangement	Type	Melanosome Dimensions
A	Individually Dispersed	$0.69\,\mu m \times 0.28\,\mu m$
B	Melanosome Complexes	$0.53\,\mu m \times 0.27\,\mu m$
C	Melanosome Complexes	$0.41\,\mu m \times 0.17\,\mu m$

reported in the literature [16], while melanosome complexes are modeled as spheres as also indicated in the literature [14]. For arrangement B, the sphere diameter is set to be equal to the major axis of the spheroids representing the encapsulated melanosomes, while for arrangement C it is set be twice the major axis of the spheroids. These choices are also based on data provided in the literature [15], [16].

The remaining parameter values used to characterize the skin specimens considered in this work are provided in Table II. We remark that these values were also selected based on actual biophysical ranges provided by scientific sources, which are listed elsewhere [23] for conciseness.

Using the datasets provided in Tables I and II, we employed HyLIoS to compute the baseline SB absorptance curves associated with the three melanosome arrangements. Within the HyLIoS' stochastic formulation, a light ray interacting with a given skin specimen can be associated with any selected wavelength within a spectral region of interest. Hence, this model can provide radiometric curves with different spectral resolutions. For consistency, however, we considered a spectral resolution of 5 nm in all absorptance curves depicted in this work. These curves were obtained using a virtual spectrophotometer [24] with the following specifications: angle of incidence equal to 0° (to minimize surface reflectance [22]) and 10^6 sample rays per wavelength (to obtain asymptotically convergent results [24]).

We have performed three sets of controlled *in silico* experiments in which we considered distinct specimens resulting from changes in selected pigmentation parameters. In the first set, we compared the baseline SB absorptance curves with SB absorptance curves computed considering the percentage of stratum basale occupied by melanosomes multiplied by a factor of 4. In the second set, we increased the SB colloidal melanin content by a factor of 4 and repeated the SB absorptance computations performed in the first set. Similarly, in the third set, we increased the concentration of eumelanin and pheomelanin in the melanosomes to 90 g/L and 4 g/L, respectively, and repeated the absorptance computations performed in the first set.

To enable the full reproduction of our *in silico* experimental results, we made HyLIoS available online [25] via a model distribution system [26] along with the supporting data (*e.g.*, refractive index and extinction coefficient curves) [27] used in our investigation. This system enables researchers to specify the values to be assigned to the measurement variables (*e.g.*, angle of incidence and spectral range) and specimen characterization parameters (*e.g.*, pigments content and melanosome dimensions) using a web interface [25], and receive customized simulation results.

TABLE II

PARAMETERS EMPLOYED IN THE CHARACTERIZATION OF THE SKIN SPECIMENS CONSIDERED IN THIS INVESTIGATION. THE ACRONYMS SC, SG, SS, SB, PD AND RD REFER TO THEIR MAIN LAYERS: STRATUM CORNEUM, STRATUM GRANULOSUM, STRATUM SPINOSUM, STRATUM BASALE, PAPILLARY DERMIS AND RETICULAR DERMIS, RESPECTIVELY.

Parameter	Value
Aspect Ratio of Skin Surface Folds	0.1
SC Thickness (cm)	0.0004
SG Thickness (cm)	0.0033
SS Thickness (cm)	0.0033
SB Thickness (cm)	0.0033
PD Thickness (cm)	0.02
RD Thickness (cm)	0.125
SC Melanosome Content (%)	0.0
SG Melanosome Content (%)	0.0
SS Melanosome Content (%)	0.0
SB Melanosome Content (%)	2.5
SC Colloidal Melanin Content (%)	0.0
SG Colloidal Melanin Content (%)	1.35
SS Colloidal Melanin Content (%)	1.35
SB Colloidal Melanin Content (%)	1.35
Melanosome Eumelanin Concentration (g/L)	32.0
Melanosome Pheomelanin Concentration (g/L)	2.0
PD Blood Content (%)	0.3
RD Blood Content (%)	0.3
Dermal Oxyhemoglobin Fraction (%)	75
Functional Hemoglobin Concentration in Blood (g/L)	147.0
Methemoglobin Concentration in Blood (g/L)	1.5
Carboxyhemoglobin Concentration in Blood (g/L)	1.5
Sulfhemoglobin Concentration Blood (g/L)	0.0
Blood Bilirubin Concentration (g/L)	0.003
SC Beta-Carotene Concentration (g/L)	2.1E-4
Epidermis Beta-Carotene Concentration (g/L)	2.1E-4
Blood Beta-Carotene Concentration (g/L)	7.0E-5
SC Water Content (%)	35.0
Epidermis Water Content (%)	60.0
PD Water Content (%)	75.0
RD Water Content (%)	75.0
SC Lipid Content (%)	20.0
Epidermis Lipid Content (%)	15.1
PD Lipid Content (%)	17.33
RD Lipid Content (%)	17.33
SC Keratin Content (%)	65.0
SC Urocanic Acid Density (mol/L)	0.01
Skin DNA Density (g/L)	0.185
SC Refractive Index	1.55
Epidermis Refractive Index	1.4
PD Refractive Index	1.39
RD Refractive Index	1.41
Melanin Refractive Index	1.7
PD Scatterers Refractive Index	1.5
Radius of PD Scatterers (nm)	40.0
PD Fraction Occupied by Scatterers (%)	22.0

For completeness, we also provide the mean relative difference (MRD) between the absorptance curves computed for the distinct melanosome arrangements during each set of our *in silico* experiments. This quantity is expressed as:

$$MRD = \frac{1}{N}\sum_{i=1}^{N}\frac{|\alpha_j(\lambda_i) - \alpha_k(\lambda_i)|}{\alpha_j(\lambda_i)} \times 100 \ (\%), \quad (1)$$

where α_j and α_k correspond to the SB absorptance curves obtained for melanosome arrangements j and k, respectively, and N is the total number of wavelengths sampled with a 5 nm resolution within the selected spectral region.

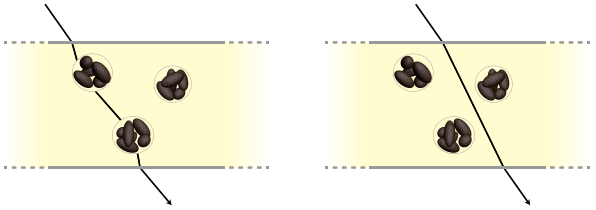

Fig. 2. Sketches illustrating detour (left) and sieve (right) effects that may take place when light traverses an epidermal layer containing melanosome complexes. The same phenomena may take place in a layer occupied by individually dispersed melanosomes.

III. RESULTS AND DISCUSSION

When light traverses a turbid medium (*e.g.*, the stratum basale), refractive index differences between the pigment-containing structures (*e.g.*, melanosome or melanosome complexes) and the surrounding medium may cause multiple interactions that increase the light optical path length, a phenomenon known as detour effect [28] (Fig. 2 (left)). Conversely, the traversing light may undergo a sieve effect, *i.e.*, it may not encounter a pigment-containing structure [29] (Fig. 2 (right)). While the former increases the probability of light absorption by the encapsulated pigment of interest, notably in bands of absorption minima, in comparison with a homogeneous solution with equal concentration of this pigment [28], the latter reduces the probability of light absorption, notably in bands of absorption maxima [30]. The net result of these effects depends on the absorption spectra of the pigments as well as on the distribution and volume fraction of these structures [28], [29]. In our experiments, the pigments of interest are the melanins, whose absorption spectra decrease monotonically in the 280-380 nm range [7].

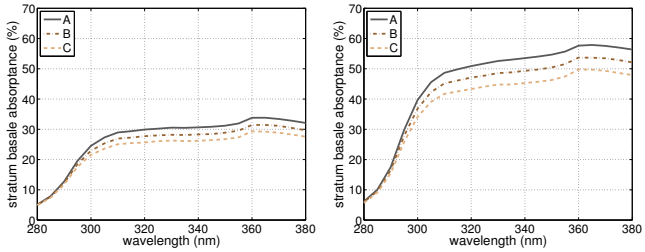

Fig. 3. Graphs depicting stratum basale (SB) absorptance curves computed considering the three melanosome arrangements (A, B and C). Left: 2.5% of the SB occupied by melanosomes. Right: 10% of the SB occupied by melanosomes. These curves were obtained using the HyLIoS model [22], [25] and, unless otherwise stated, the data provided in Tables I and II.

TABLE III

MEAN RELATIVE DIFFERENCE (MRD) VALUES COMPUTED FOR THE STRATUM BASALE ABSORPTANCE CURVES DEPICTED IN FIG. 3.

Melanosome Arrangements	Left Graph		Right Graph	
	UVB	UVA	UVB	UVA
A & B	5.36%	7.36%	6.21%	7.50%
B & C	5.01%	7.13%	6.62%	7.89%

The SB absorptance curves obtained in our first set of experiments (Fig. 3) indicate that large and individually dispersed melanosomes (arrangement A) absorb light more

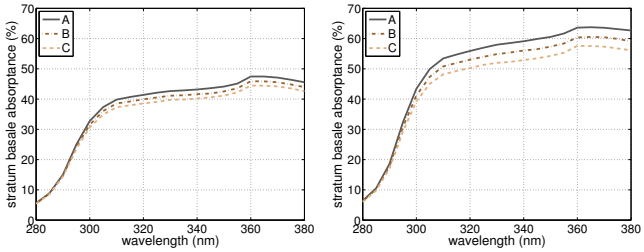

Fig. 4. Graphs depicting stratum basale (SB) absorptance curves computed considering the three melanosome arrangements (A, B and C) and the SB colloidal melanin content increased to 5.4%. Left: 2.5% of the SB occupied by melanosomes. Right: 10% of the SB occupied by melanosomes. These curves were obtained using the HyLIoS model [22], [25] and, unless otherwise stated, the data provided in Tables I and II.

TABLE IV

MEAN RELATIVE DIFFERENCE (MRD) VALUES COMPUTED FOR THE STRATUM BASALE ABSORPTANCE CURVES DEPICTED IN FIG. 4.

Melanosome Arrangements	Left Graph		Right Graph	
	UVB	UVA	UVB	UVA
A & B	2.92%	3.55%	4.44%	5.25%
B & C	2.56%	3.21%	4.55%	5.19%

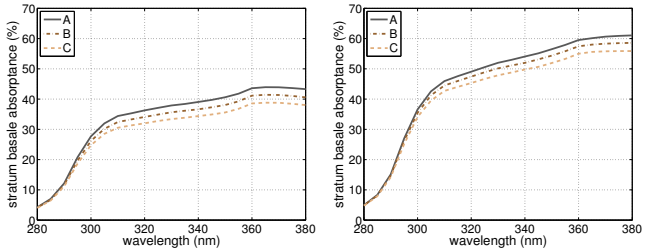

Fig. 5. Graphs depicting stratum basale (SB) absorptance curves computed considering the three melanosome arrangements (A, B and C) and the concentrations of eumelanin and pheomelanin in the organelles increased to 90 g/L and 4 g/L, respectively. Left: 2.5% of the SB occupied by melanosomes. Right: 10% of the SB occupied by melanosomes. These curves were obtained using the HyLIoS model [22], [25] and, unless otherwise stated, the data provided in Tables I and II.

TABLE V

MEAN RELATIVE DIFFERENCE (MRD) VALUES COMPUTED FOR THE STRATUM BASALE ABSORPTANCE CURVES DEPICTED IN FIG. 5.

Melanosome Arrangements	Left Graph		Right Graph	
	UVB	UVA	UVB	UVA
A & B	4.89%	5.97%	2.74%	3.61%
B & C	4.66%	6.24%	3.57%	4.43%

efficiently than melanosome complexes (arrangements B and C) formed by smaller organelles. They also indicate that more compact melanosome complexes (arrangement B) absorb light more efficiently than less compact ones (arrangement C). In addition, the absorptance curves depicted in Fig. 3 and the MRD values presented in Table III, show that an increased melanosome presence in the layer tends to increase the magnitude of these differences in absorption efficiency.

These differences are directly associated with the occurrence of detour and sieve effects. More specifically, large and individually dispersed melanosomes are more likely to be hit by traversing light rays than melanosome complexes. Accordingly, the impact of the detour effect on UVR absorption elicited by the former is more substantial than the impact elicited by the latter. Similarly, the impact of the detour effect on UVR absorption elicited by more compact melanosome complexes is more substantial than the impact elicited by less compact complexes. Furthermore, as also indicated by the MRD values presented in Table III, the impact of the detour effect is more pronounced in the UVA region, the band of absorption minima of the melanins in the ultraviolet domain. We remark that this is the band in which detour effects lead to more substantial increases in the probability of light absorption by pigments [28].

It is important to note that detour effects can lead to an absorption intensification because the concentration of the encapsulated melanin is higher than the concentration of the colloidal melanin present in the surrounding medium. Accordingly, the SB absorptance curves obtained in our second set of experiments (Fig. 4) and their corresponding MRD values (Table IV) indicate that an increase in the concentration of the surrounding colloidal melanin reduces the differences in absorption efficiency among the distinct melanosome arrangements. In this case, the relative contribution of the melanosomes for the total absorption occurring in the layer is reduced by the larger contribution provided by the colloidal melanin. Moreover, the increased presence of colloidal melanin also reduces the impact of detour effects since light rays that do not encounter the melanosomes have a higher probability of being absorbed while traversing the surrounding medium.

The SB absorptance curves obtained in our third set experiments (Fig. 5) also indicate differences in absorption efficiency among the distinct melanosome arrangements when the concentration of the encapsulated melanins is increased. In this case, however, an increased presence of melanosomes (Fig. 5 (right)) is not followed by larger differences in absorption efficiency as observed when we considered a smaller concentration for the encapsulated melanin (Fig. 3 (right)). In fact, in this case, the differences tend to become smaller as it can also be verified by comparing the corresponding MRD values presented in Tables III and V. From a tissue optics perspective, the presence of larger number of melanosomes, or melanosome complexes, increases the probability of more melanosome-ray interactions taking place along a ray trajectory, which would increase its path length. When the concentration of the encapsulated melanin is significantly high, however, the probability of a ray to be absorbed after a few hits increases as well. Thus, in this case, the differences in absorption efficiency associated with the detour effect tend to be reduced among the distinct melanosome arrangements for both small and large percentages of the SB occupied by melanosomes.

In short, our experimental results quantitatively demonstrate for the first time the different levels of UVR attenuation provided by distinct melanosome arrangements in conjunction with variations in pigmentation parameters. More specifically, they indicate a superior level of UVR

attenuation by large and individually dispersed melanosomes over melanosome complexes, and a superior level of UVR attenuation by compact melanosome complexes over larger complexes formed by smaller melanosomes. In addition, such superiorities are more significant in the UVA spectral region than in the UVB. Our results also indicate that these differences in absorption efficiency among the distinct melanosome arrangements are mitigated by an increased presence of colloidal melanin and/or higher concentrations of the encapsulated melanin.

IV. Conclusion

The correct interpretation of skin pigmentation data is essential when performing a noninvasive assessment of an individual's susceptibility to develop UVR-induced pathologies, particularly those with a relatively high mortality rate such as melanoma skin cancer. Viewed in this context, besides their biophysical significance, our findings underscore the importance of accounting for all relevant light attenuation processes taking place within the cutaneous tissues, and contribute for enhancing the efficacy of these assessments. For example, most sunscreens are designed to protect us against sunburn caused by UVB exposure. In fact, a sunscreen SPF (Sun Protection Factor) specifically indicates protection against UVB [31]. However, UVA (which corresponds to about 95% of the UVR present in ambient sunlight [3]) can also lead to skin cancer, immunosuppression and photoaging [2], [3], [4]. Our findings show that UVA corresponds to the spectral region more susceptible to different levels of UVR absorption efficiency elicited by distinct melanosome arrangements. Accordingly, these aspects should be taken into account in the design of sunscreens aimed to provide effective coverage for both UVB and UVA radiation.

References

[1] J. Barth, J. Cadet, J.P. Césarini, T.B. Fitzpatrick, A. McKinlay, M. Mutzhas, M. Pathak, M. Peak, D. Sliney, and F. Urbach, "CIE-134 collection in photobiology and photochemistry," in *TC6-26 report: Standardization of the Terms UV-A1, UV-A2 and UV-B*. 1999, Commission International de L'Eclairage.

[2] A. Juzeniene, P. Brekke, A. Dahlback, S. Andersson-Engels, J. Reichrath, K. Moan, M.F. Holick, W.B. Grant, and J. Moan, "Solar radiation and human health," *Reports on Progress in Physics*, vol. 74, no. 6, pp. 066701, 2011.

[3] L.S. Sklar, F. Almutawa, H.W. Lim, and I. Hamzavi, "Effects of ultraviolet radiation, visible light, and infrared radiation on erythema and pigmentation: a review," *Photochem. Photobiol. Sci.*, vol. 12, pp. 54–64, 2013.

[4] G.J. Clydesdale, G.W. Dandie, and H.K. Muller, "Ultraviolet light induced injury: immunological and inflammatory effects," *Immunol. Cell. Biol.*, vol. 79, no. 6, pp. 547– 568, 2001.

[5] A.R. Young, "Chromophores in human skin," *Physics in Medicine and Biology*, vol. 42, no. 5, pp. 789, 1997.

[6] M. Brenner and V.J. Hearing, "The protective role of melanin against UV damage in human skin," *Photochem. Photobiol.*, vol. 84, no. 3, pp. 539–549, 2008.

[7] T. Sarna and H.M. Swartz, "The physical properties of melanins," in *The Pigmentary System Physiology and Pathophysiology*, J.J. Nordlund, R.E. Boissy, V.J. Hearing, R.A. King, and J.P. Ortonne, Eds., New YorK, NY, USA, 2006, pp. 311–341, Oxford University Press.

[8] Y. Miyamura, S.G. Coelho, K. Schlenz, J. Batzer, C. Smuda, W. Choi, M. Brenner, T. Passeron, G. Zhang, L. Kolbe, R. Wolber, and V.J. Hearing, "The deceptive nature of UVA tanning versus the modest protective effects of UVB tanning on human skin," *Pigm. Cell Mel*, vol. 24, pp. 136–147, 2010.

[9] M.A. Pathak, "Functions of melanin and protection by melanin," in *Melanin: Its Role in Human Photoprotection*, L. Zeise, M.R. Chedekel, and T.B. Fitzpatrick, Eds., Overland Park, Kansas, USA, 1995, pp. 125–134, Valdenmar Publishing Co.

[10] Y. Miyamura, S.G. Coelho, R. Wolber, S.A. Miller, K. Wakamatsu, B.Z. Zmudzka, S. Ito, C. Smuda, T. Passeron, W. Choi, J. Batzer, Y. Yamaguchi, J.Z. Beer, and V.J. Hearing, "Regulation of human skin pigmentation and responses to ultraviolet radiation," *Pigm. Cell Res.*, vol. 20, no. 1, pp. 2–13, 2006.

[11] R.R. Anderson and J.A. Parrish, "Optical properties of human skin," in *The Science of Photomedicine*, J.D. Regan and J.A. Parrish, Eds., N.Y., USA, 1982, pp. 147–194, Plenun Press.

[12] K.P. Nielsen, L. Zhao, J.J. Stamnes, K. Stamnes, and J. Moan, "The importance of the depth distribution of melanin in skin for DNA protection and other photobiological processes," *J. Photoch. Photobio. B.*, vol. 82, no. 3, pp. 194–198, 2006.

[13] T.F. Chen and G.V.G Baranoski, "On the detection of peripheral cyanosis in individuals with distinct levels of cutaneous pigmentation," in *37th International Conference of the IEEE Engineering in Medicine and Biology Society (EMBC)*. IEEE, 2015, pp. 4415–4418.

[14] N. Kollias, R.M. Sayre, L. L. Zeise, and M.R. Chedekel, "Photoprotection by melanin," *J. Photoch. Photobio. B.*, vol. 9, no. 2, pp. 135–60, 1991.

[15] G. Szabo, A. Gerald, M. Pathak, and T.B. Fitzpatrick, "Racial differences in the fate of melanosomes in human epidermis," *Nature*, vol. 222, no. 5198, pp. 1081–1082, 06 1969.

[16] R.L. Olson, J. Gaylor, and M.A. Everett, "Skin color, melanin, and erythema," *Arch. Dermatol.*, vol. 108, no. 4, pp. 541–544, 1973.

[17] H.Y. Thong, S.H. Jee, C.C. Sun, and R.E. Boissy, "The patterns of melanosome distribution in keratinocytes of human skin as one determining factor of skin color," *Br. J. Dermatol.*, vol. 149, pp. 498–505, 2003.

[18] K.H. Kaidbey, P.P. Agin, R.M. Sayre, and A.M. Kligman, "Photoprotection by melanin - a comparison of black and caucasian skin," *J. Am. Acad. Dermatol.*, vol. 1, pp. 249–260, 1979.

[19] Y. Yamaguchi, M. Brenner, and V. J. Hearing, "The regulation of skin pigmentation," *J. Biol. Chem.*, vol. 282, no. 38, pp. 27557–27561, 2007.

[20] S. Alaluf, D. Atkins, K. Barret, M. Blount, N. Carter, and A. Heath, "Ethnic variation in melanin content and composition in photoexposed and photoprotected human skin," *Pigment Cell Res.*, vol. 15, pp. 112–118, 2002.

[21] R.E. Mitchell, "The skin of the Australian Aborigine; a light and electronmicroscopical study," *Austral. J. Dermatol.*, vol. 9, no. 4, pp. 414–328, 1968.

[22] T.F. Chen, G.V.G. Baranoski, B.W. Kimmel, and E. Miranda, "Hyperspectral modeling of skin appearance," *ACM Trans. Graph.*, vol. 34, no. 3, pp. 31:1–31:14, 2015.

[23] G.V.G Baranoski, S.R. Van Leeuwen, and T.F. Chen, "On the detection of peripheral cyanosis in individuals with distinct levels of cutaneous pigmentation," in *39th International Conference of the IEEE Engineering in Medicine and Biology Society (EMBC)*. IEEE, 2017, pp. 4260–4264.

[24] G.V.G. Baranoski, J.G. Rokne, and G. Xu, "Virtual spectrophotometric measurements for biologically and physically-based rendering," *The Visual Computer*, vol. 17, no. 8, pp. 506–518, 2001.

[25] Natural Phenomena Simulation Group (NPSG), *Run HyLIoS Online*, School of Computer Science, University of Waterloo, Ontario, Canada, 2017, http://www.npsg.uwaterloo.ca/models/hyliosEx.php.

[26] G.V.G. Baranoski, T. Dimson, T.F. Chen, B. Kimmel, D. Yim, and E. Miranda, "Rapid dissemination of transport models on the web," *IEEE Computer Graphics & Applications*, vol. 32, pp. 10–15, 2012.

[27] NPSG, *Human Skin Data*, Natural Phenomena Simulation Group (NPSG), School of Computer Science, University of Waterloo, Ontario, Canada, 2014, http://www.npsg.uwaterloo.ca/data/skin.php.

[28] W.L. Butler, "Absorption spectroscopy *in vivo*: theory and application," *Annu. Rev. Plant Phys.*, vol. 15, pp. 451–470, 1964.

[29] L. Fukshansky, "Absorption statistics in turbid media," *J. Quant. Spectrosc. Radiat. Transfer*, vol. 38, pp. 389–406, 1987.

[30] P. Latimer, "A wave-optics effect which enhances light absorption by chlorophyll *in vivo*," *Photochem. Photobiol.*, vol. 40, no. 2, pp. 193–199, 1984.

[31] E. Questel and Y. Gall, "Photobiological assessment of sunscreens," in *Measuring the Skin*, P. Agache and P. Humbert, Eds., Berlin, 2004, pp. 492–505, Springer-Verlag.